Title
SOURCE PROVENANCE OF OBSIDIAN ARTIFACTS FROM CA-KER-8146 AND 10683 ON THE NAVAL AIR WEAPONS STATION CHINA LAKE, INYO COUNTY, CALIFORNIA

Author
Shackley, M. Steven

Publication Date
2021-06-08

GEOARCHAEOLOGICAL XRF LAB
A GREEN SOLAR FACILITY

GEOARCHAEOLOGICAL X-RAY FLUORESCENCE SPECTROMETRY LABORATORY
8100 Wyoming Blvd., Ste M4-158 Albuquerque, NM 87113
USA

SOURCE PROVENANCE OF OBSIDIAN ARTIFACTS FROM CA-KER-8146 AND 10683 ON THE NAVAL AIR WEAPONS STATION CHINA LAKE, INYO COUNTY, CALIFORNIA

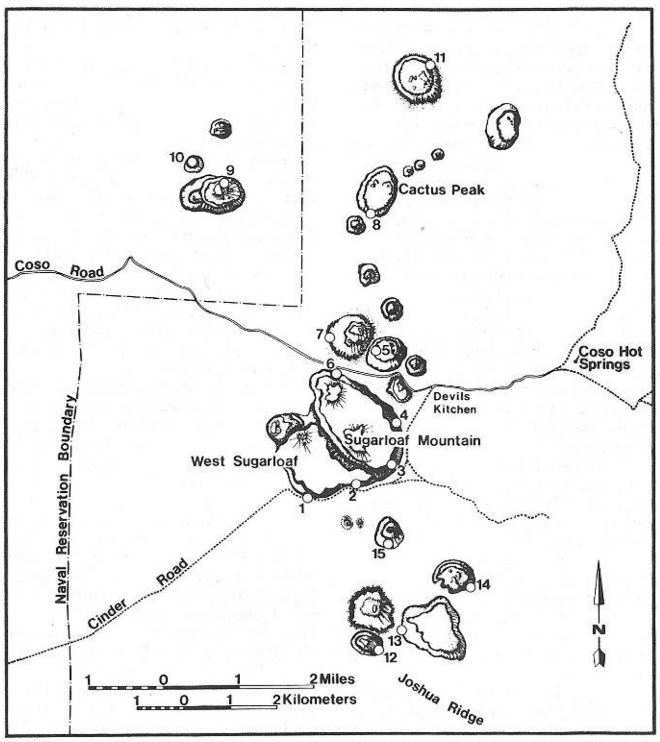

A portion of the Coso Volcanic Field with relevant rhyolite domes (from Bacon et al. 1981; Hughes 1988)

by

M. Steven Shackley, Ph.D., Director
Geoarchaeological XRF Laboratory
Albuquerque, New Mexico

Report Prepared for

Epsilon Systems Solutions, Inc.
Ridgecrest, California

8 June 2021

INTRODUCTION

The analysis here of 52 obsidian artifacts from two archaeological sites within the China Lake Naval Weapons Station, as in many of the previous studies, indicated the presence of mainly Coso Volcanic Field obsidian sources (Hughes 1988; Ericson and Glascock 2004; Shackley 2014, 2015a, 2015b, 2016, 2017, 2019a, 2019b). As typical for sites on the weapons station, the assemblage is dominated by artifacts produced from the West Sugarloaf dome, followed by Sugarloaf and West Cactus Peak (Table 1 and Figure 1). While there has been some argument that differential procurement of the Coso sources is not necessarily socially important, the work of Eerkens and Rosenthal at Coso suggests that there is some selection that may be socially significant (2004). Unlike previous studies, however, two artifacts from CA-KER-8146 were produced from two of the localities at Casa Diablo in east-central California (Hughes 1994; Table 1 and Figure 1 herein).

LABORATORY SAMPLING, ANALYSIS AND INSTRUMENTATION

All archaeological samples are analyzed whole. The results presented here are quantitative in that they are derived from "filtered" intensity values ratioed to the appropriate x-ray continuum regions through a least squares fitting formula rather than plotting the proportions of the net intensities in a ternary system (McCarthy and Schamber 1981; Schamber 1977). Or more essentially, these data through the analysis of international rock standards, allow for inter-instrument comparison with a predictable degree of certainty (Hampel 1984; Shackley 2011).

All analyses for this study were conducted on a ThermoScientific *Quant'X* EDXRF spectrometer, located at the Geoarchaeological XRF Laboratory, Albuquerque, New Mexico. It is equipped with a thermoelectrically Peltier cooled solid-state Si(Li) X-ray detector, with a 50 kV, 50 W, ultra-high-flux end window bremsstrahlung, Rh target X-ray tube and a 76 µm (3 mil) beryllium (Be) window (air cooled), that runs on a power supply operating 4-50 kV/0.02-1.0 mA at 0.02 increments. The spectrometer is equipped with a 200 l min^{-1} Edwards vacuum pump, allowing for the analysis of lower-atomic-weight elements between sodium (Na) and titanium (Ti). Data acquisition is accomplished with a pulse processor and an analogue-to-digital converter. Elemental composition is identified with digital filter background removal, least squares empirical peak deconvolution, gross peak intensities and net peak intensities above background.

For the analysis of mid Zb condition elements Ti-Nb, Pb, Th, the x-ray tube is operated at 30 kV, using a 0.05 mm (medium) Pd primary beam filter in an air path at 100 seconds livetime to generate x-ray intensity $K\alpha_1$-line data for elements titanium (Ti), manganese (Mn), iron (as $Fe_2O_3^T$), cobalt (Co), nickel (Ni), copper, (Cu), zinc, (Zn), gallium (Ga), rubidium (Rb), strontium (Sr), yttrium (Y), zirconium (Zr), niobium (Nb), and $L\alpha_1$-line data for lead (Pb), and thorium (Th). Not all these elements are reported since their values in many volcanic rocks are very low. Trace element intensities were converted to concentration estimates by employing a linear calibration line ratioed to the Compton scatter established for each element from the analysis of international rock standards certified by the National Institute of Standards and Technology (NIST), the US. Geological Survey (USGS), Canadian Centre for Mineral and Energy Technology, and the Centre de Recherches Pétrographiques et Géochimiques in France (Govindaraju 1994). Line fitting is linear (XML) for all elements but Fe where a derivative fitting is used to improve the fit for iron and thus for all the other elements. When barium (Ba) is analyzed in the High Zb condition, the Rh tube is operated at 50 kV and up to 1.0 mA, ratioed to the bremsstrahlung region (see Davis 2011; Shackley 2011). Further details concerning the petrological choice of these elements in Southwest obsidians is available in Shackley (1995, 2005; also Mahood and Stimac 1991; and Hughes and Smith 1993). Nineteen specific pressed powder standards are used for the best fit regression calibration for elements Ti-Nb, Pb, Th, and Ba, include G-2 (basalt), AGV-2 (andesite), GSP-2 (granodiorite), SY-2 (syenite), BHVO-2 (hawaiite), STM-1 (syenite), QLO-1 (quartz latite), RGM-1 (obsidian), W-2 (diabase), BIR-1 (basalt), SDC-1 (mica schist), TLM-1 (tonalite), SCO-1 (shale), NOD-A-1 and NOD-P-1 (manganese) all US Geological Survey standards, NIST-278 (obsidian), U.S. National Institute of Standards and Technology, BE-N (basalt) from the Centre de Recherches Pétrographiques et Géochimiques in France, and JR-1 and JR-2 (obsidian) from the Geological Survey of Japan

(Govindaraju 1994). RGM-1 a USGS obsidian standard from Glass Mountain, Medicine Lake Highlands is analyzed during each sample run of ≤ 19 to check stability of machine calibration (Table 1). Source assignments were made by comparison to Ericson and Glascock (2004) and Hughes (1988; see Table 1 and Figure 1 here), as well as source standards for Sugarloaf, West Sugarloaf, and West Cactus Peak in this laboratory. Statistical data analysis progressed through Excel to JMP 12.0.1.

REFERENCES CITED

Bacon, C.R., R. Macdonald, R.L. Smith, and P.A. Baedecker
1981 *Pleistocene High-Silica Rhyolites of the Coso Formation, Inyo County, California*. U.S. Geological Survey Bulletin 1527.

Davis, M.K., T.L. Jackson, M.S. Shackley, T. Teague, and J. Hampel
2011 Factors Affecting the Energy-Dispersive X-Ray Fluorescence (EDXRF) Analysis of Archaeological Obsidian. In *X-Ray Fluorescence Spectrometry (XRF) in Geoarchaeology*, edited by M.S. Shackley, pp. 45-64. Springer, New York.

Eerkens, J.W., and J. S. Rosenthal
2004 Are Obsidian Subsources Meaningful Units of Analysis?: Temporal and Spatial Patterning of Subsources in the Coso Volcanic Field, Southeastern California. *Journal of Archaeological Science* 31:21-29.

Ericson, J.E., and M.D. Glascock
2004 Subsource Characterization: Obsidian Utilization of Subsources of the Coso Volcanic Field, Coso Junction, California, USA. *Geoarchaeology* 19:779-805.

Govindaraju, K.
1994 1994 Compilation of Working Values and Sample Description for 383 Geostandards. *Geostandards Newsletter* 18 (special issue).

Hampel, Joachim H.
1984 Technical Considerations in X-ray Fluorescence Analysis of Obsidian. In *Obsidian Studies in the Great Basin*, edited by R.E. Hughes, pp. 21-25. Contributions of the University of California Archaeological Research Facility 45. Berkeley.

Hildreth, W.
1981 Gradients in Silicic Magma Chambers: Implications for Lithospheric Magmatism. *Journal of Geophysical Research* 86:10153-10192.

Hughes, Richard E.
1988 The Coso Volcanic Field Reexamined: Implications for Obsidian Sourcing and Hydration Dating Research. *Geoarchaeology* 3:253-265.

1994 Intrasource Chemical Variability of Artefact-Quality Obsidians from the Casa Diablo Area, California. *Journal of Archaeological Science* 21:263-271)

Hughes, Richard E., and Robert L. Smith
1993 Archaeology, Geology, and Geochemistry in Obsidian Provenance Studies. *In Scale on Archaeological and Geoscientific Perspectives*, edited by J.K. Stein and A.R. Linse, pp. 79-91. Geological Society of America Special Paper 283.

Mahood, Gail A., and James A. Stimac
1990 Trace-Element Partitioning in Pantellerites and Trachytes. *Geochemica et Cosmochimica Acta* 54:2257-2276.

McCarthy, J.J., and F.H. Schamber
1981 Least-Squares Fit with Digital Filter: A Status Report. In *Energy Dispersive X-ray Spectrometry*, edited by K.F.J. Heinrich, D.E. Newbury, R.L. Myklebust, and C.E. Fiori, pp. 273-296. National Bureau of Standards Special Publication 604, Washington, D.C.

Schamber, F.H.
1977 A Modification of the Linear Least-Squares Fitting Method which Provides Continuum Suppression. In *X-ray Fluorescence Analysis of Environmental Samples*, edited by T.G. Dzubay, pp. 241-257. Ann Arbor Science Publishers.

Shackley, M. Steven
1995 Sources of Archaeological Obsidian in the Greater American Southwest: An Update and Quantitative Analysis. *American Antiquity* 60(3):531-551.

2005 *Obsidian: Geology and Archaeology in the North American Southwest*. University of Arizona Press, Tucson.

2011 An Introduction to X-Ray Fluorescence (XRF) Analysis in Archaeology. In *X-Ray Fluorescence Spectrometry (XRF) in Geoarchaeology*, edited by M.S. Shackley, pp. 7-44. Springer, New York.

2014 Source Provenance of Obsidian Artifacts from Five Sites on the Naval Weapons Station China Lake, Inyo, Kern, and San Bernardino Counties, California. Report prepared for Epsilon Systems Solutions, Ridgecrest, California.

2015a An Energy-Dispersive X-Ray Fluorescence Analysis of Obsidian Artifacts from Site Cs-Tl-01 on the Coles Sam Road Project, Naval Weapons Station China Lake, Inyo County, California. Report prepared for Epsilon Systems Solutions, Ridgecrest, California.

2015b Source Provenance of Obsidian Artifacts from Two Sites on the Naval Weapons Station China Lake, Inyo, Kern, and San Bernardino Counties, California. Report prepared for Epsilon Systems Solutions, Ridgecrest, California.

2016 Source Provenance Of Obsidian Artifacts from 25 Sites on the Naval Weapons Station China Lake, Inyo, Kern County, California. Report prepared for Epsilon Systems Solutions, Ridgecrest, California.

2017 Source Provenance Of Obsidian Artifacts from Archaeological Sites on the Naval Weapons Station China Lake, Inyo, Kern, and San Bernardino Counties, California. Report prepared for Epsilon Systems Solutions, Ridgecrest, California.

2019a Source Provenance of Obsidian Artifacts from CA-INY-7833 on the Naval Air Weapons Station China Lake, Inyo County, California. Report prepared for Epsilon Systems Solutions, Ridgecrest, California.

2919b Source Provenance of Obsidian Artifacts from G4-DM-02 and G4-DM-03 on the Naval Air Weapons Station China Lake, Inyo County, California. Report prepared for Epsilon Systems Solutions, Ridgecrest, California.

Table 1. Elemental concentrations and source assignments for the samples and USGS RGM-1 rhyolite standard. All measurements in parts per million (ppm).

Sample	Site	Ti	Mn	Fe	Zn	Rb	Sr	Y	Zr	Nb	Ba	Pb	Th	Source
4A	KER-8146	583	290	11960	130	258	17	55	137	45		26	34	West Sugarloaf
6	KER-8146	578	312	12604	131	297	16	55	143	53		38	44	West Sugarloaf
8	KER-8146	513	313	12916	129	229	16	43	163	38		28	32	West Sugarloaf
10	KER-8146	638	308	11816	103	256	18	57	130	50		31	39	West Sugarloaf
11A	KER-8146	644	302	12313	98	278	16	52	143	50		33	47	West Sugarloaf
11B	KER-8146	617	300	12273	143	284	14	53	144	40		39	44	West Sugarloaf
13A	KER-8146	616	270	11947	72	187	16	40	163	35		23	26	West Sugarloaf
13B	KER-8146	633	315	12550	97	214	20	43	163	32		25	32	West Sugarloaf
14A	KER-8146	619	268	12043	61	201	17	52	156	34		25	39	West Sugarloaf
45	KER-8146	682	290	12195	118	271	16	57	142	50		29	37	West Sugarloaf
46	KER-8146	553	359	12323	154	283	12	51	116	44		46	49	West Cactus Peak
47A	KER-8146	550	292	12263	100	194	17	40	146	37		29	32	West Sugarloaf
49	KER-8146	625	313	12342	194	278	13	50	145	38		38	40	West Sugarloaf
50	KER-8146	606	373	12845	165	291	14	52	125	46		40	46	West Cactus Peak
50A	KER-8146	794	299	11743	151	175	17	39	162	31		21	31	West Sugarloaf
56	KER-8146	611	317	12381	108	290	16	56	153	51		32	39	West Sugarloaf
58	KER-8146	891	298	12250	165	235	15	48	141	38		29	29	West Sugarloaf

62A	KER-8146	563	284	12170	65	240	19	50	155	43		28	37	West Sugarloaf
70	KER-8146	808	281	12086	129	275	13	55	159	47		34	28	West Sugarloaf
70A	KER-8146	844	315	11959	140	252	13	52	112	43		35	43	Sugarloaf
74	KER-8146	526	320	12498	89	305	17	54	153	49		35	35	West Sugarloaf
75A	KER-8146	1419	329	13025	45	164	129	17	207	15	1508	28	24	Sawmill Ridge (Casa Diablo)
75B	KER-8146	452	304	12269	109	298	20	54	144	41		31	43	West Sugarloaf
76	KER-8146	608	281	12109	61	197	19	45	159	32		22	25	West Sugarloaf
79	KER-8146	613	303	12589	90	204	17	46	156	38		25	41	West Sugarloaf
80A	KER-8146	518	297	11856	132	258	16	48	143	44		30	27	West Sugarloaf
81A	KER-8146	661	325	12668	71	274	15	56	148	44		32	40	West Sugarloaf
81B	KER-8146	718	272	12367	105	185	24	46	144	38		27	18	West Sugarloaf
81C	KER-8146	796	315	12384	137	270	15	53	137	39		34	31	West Sugarloaf
85	KER-8146	736	352	13088	132	288	14	59	145	49		37	37	West Sugarloaf
87	KER-8146	733	318	13068	84	258	27	50	165	41		32	37	West Sugarloaf
Sample	Site	Ti	Mn	Fe	Zn	Rb	Sr	Y	Zr	Nb	Ba	Pb	Th	Source
144A	KER-8146	603	322	12577	120	289	16	62	147	48		37	48	West Sugarloaf
144B	KER-8146	510	292	11931	109	273	16	51	140	45		32	29	West Sugarloaf
145	KER-8146	541	326	12531	112	279	20	54	153	49		36	33	West Sugarloaf
146A	KER-8146	535	327	12636	141	306	18	56	149	55		38	39	West Sugarloaf
147	KER-8146	151	311	1305	17	146	94	16	170	12	994	37	17	Lookout Mtn (Casa

		0		0	9									Diablo)
3A	KER-8146	552	290	12258	110	286	17	53	143	48		33	45	West Sugarloaf
4	KER-10683	532	295	12161	67	277	16	56	146	46		28	39	West Sugarloaf
6	KER-10683	579	285	11894	59	193	13	45	149	35		26	24	West Sugarloaf
7	KER-10683	612	303	12114	95	271	17	60	140	45		35	28	West Sugarloaf
9	KER-10683	482	286	12295	109	291	17	60	142	48		37	39	West Sugarloaf
10	KER-10683	603	296	12374	79	236	21	47	154	44		26	28	West Sugarloaf
11	KER-10683	597	305	11994	101	272	15	55	142	48		31	41	West Sugarloaf
13	KER-10683	525	308	12131	83	277	15	56	139	50		35	41	West Sugarloaf
13A	KER-10683	503	279	11933	83	259	17	51	135	51		35	46	West Sugarloaf
15	KER-10683	563	278	11848	66	220	19	48	147	44		29	40	West Sugarloaf
17	KER-10683	673	291	12046	72	273	14	59	149	50		31	39	West Sugarloaf
18	KER-10683	502	299	11734	65	264	13	52	141	51		32	30	West Sugarloaf
18A	KER-10683	617	296	12338	90	270	17	60	149	50		35	30	West Sugarloaf
21	KER-10683	797	333	12962	157	292	15	51	141	38		41	46	West Sugarloaf
23	KER-10683	506	297	11758	103	265	14	56	139	48		32	28	West Sugarloaf
24	KER-10683	592	321	12470	126	297	17	62	143	52		40	52	West Sugarloaf
RGM1-S4		1494	302	13591	39	145	107	20	216	13		17	19	
RGM1-S4		1375	295	13695	43	150	106	26	224	12	808	21	21	

Table 2. Crosstabulation of site by source.

			Site		
			KER-10683	KER-8146	Total
Source	West Sugarloaf	Count	15	32	47
		% within Source	31.9%	68.1%	100.0%
		% within Site	100.0%	86.5%	90.4%
		% of Total	28.8%	61.5%	90.4%
	West Cactus Peak	Count	0	2	2
		% within Source	0.0%	100.0%	100.0%
		% within Site	0.0%	5.4%	3.8%
		% of Total	0.0%	3.8%	3.8%
	Sugarloaf	Count	0	1	1
		% within Source	0.0%	100.0%	100.0%
		% within Site	0.0%	2.7%	1.9%
		% of Total	0.0%	1.9%	1.9%
	Lookout Mtn (Casa Diablo)	Count	0	1	1
		% within Source	0.0%	100.0%	100.0%
		% within Site	0.0%	2.7%	1.9%
		% of Total	0.0%	1.9%	1.9%
	Sawmill Ridge (Casa Diablo)	Count	0	1	1
		% within Source	0.0%	100.0%	100.0%
		% within Site	0.0%	2.7%	1.9%
		% of Total	0.0%	1.9%	1.9%
Total		Count	15	37	52
		% within Source	28.8%	71.2%	100.0%
		% within Site	100.0%	100.0%	100.0%
		% of Total	28.8%	71.2%	100.0%

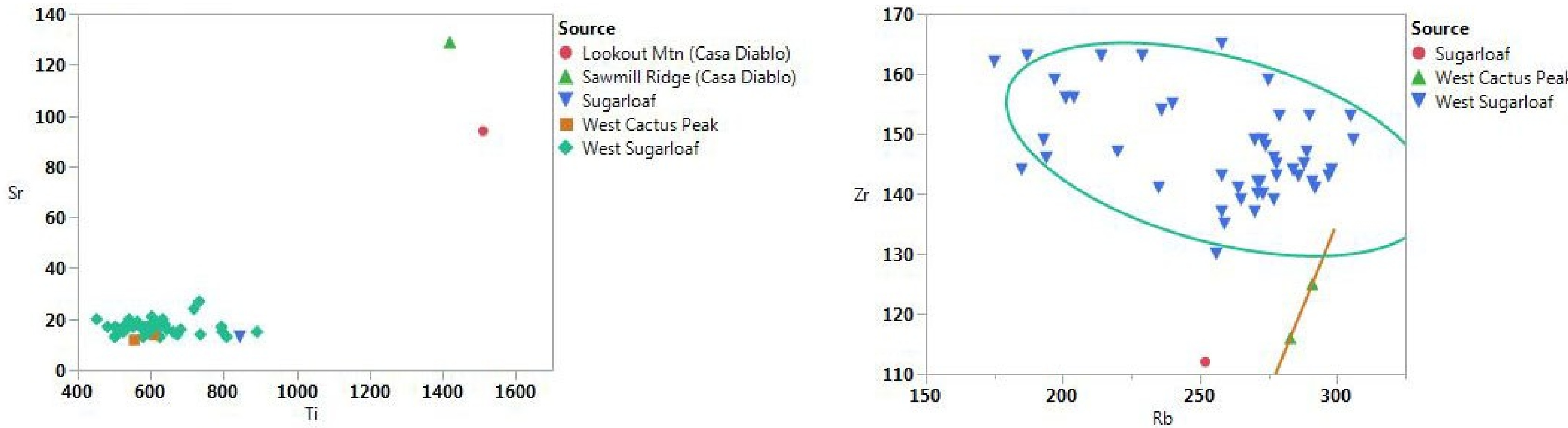

Figure 1. Ti/Sr bivariate plot of all the archaeological samples discriminating the Casa Diablo samples - left (after Hughes 1994:268). Rb/Zr bivariate plot of the Coso Volcanic Field samples only - right (after Hughes 1988:258-259). Confidence ellipse/line at 90%.